JACS
JOURNAL OF THE AMERICAN CHEMICAL SOCIETY
pubs.acs.org/JACS
Article

"Outlaw" Dipole-Bound Anions of Intra-Molecular Complexes

Valery F. Sidorkin,* Elena F. Belogolova, Evgeniya P. Doronina, Gaoxiang Liu, Sandra M. Ciborowski, and Kit H. Bowen*

Cite This: J. Am. Chem. Soc. 2020, 142, 2001−2011
Read Online
ACCESS | Metrics & More | Article Recommendations | Supporting Information

ABSTRACT: Using the example of silatranes $XSi(OCH_2CH_2)_3N$ (X = Me, H, F, Cl), **XS**, it was found that the effect of the dipole-bound (DB) electron on the cage intramolecular complexes does not fit into the standard views. Upon the transition from **XS** to the DB anions $\mathbf{XS}^-$, the unusual shortening of the internuclear Si···N distance is always observed. For X = Cl, it is equal to 0.15 Å, which is a record length for all DB anions known from the literature. The formation of DB anions with the cage structure has principal features, controlled not only by the "critical" value of the dipole moment (μ > 2.5 D), but also by a geometric factor, such as the degree of pyramidality of the $N(CH_2)_3$ moiety—the positive end of the molecular dipole of **XS**. It was a surprise that the effect of the substituent X on the extent of the structural rearrangement in the process $\mathbf{XS} \rightarrow \mathbf{XS}^-$ cannot be explained using the values of the electron detachment energy of $\mathbf{XS}^-$ or the initial strength of the coordination Si ← N bond in **XS**. The unique sensitivity of the silatrane geometry to the addition of an excess electron is governed by the rate of increase of their dipole moment with the shortening of the dative Si ← N contact. The conclusions drawn are supported by the high-accuracy CCSD and CCSD(T) calculations and the experimental (RET-PES) data. There is no real reason to doubt that the peculiarities of the formation of DB anions of $\mathbf{XS}^-$ can also be characteristic of many hundreds of their structural analogues $XM(YCH_2CH_2)_3N$ (M = Si, Ge, Sn, Pb, Ti, Al, Cr, Fe, Ni...; Y = O, NR, CH_2, S), i.e., substituted 5-azabicyclo[3.3.3]undecans.

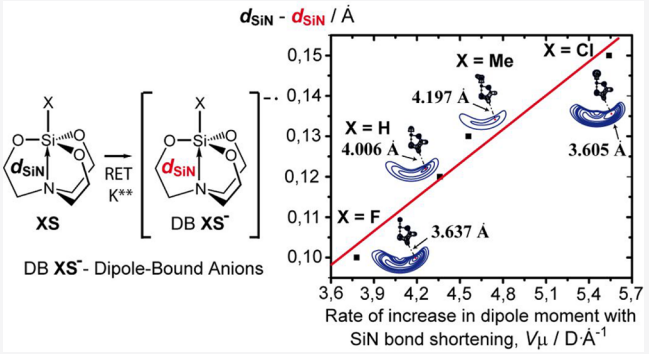

1. INTRODUCTION

The continued interest in the dipole-bound (DB) anions formed by the interaction of an excess electron with highly polar neutral molecules or clusters is due to a number of reasons.[1] Among them, there is the practical importance of studies on the structure and transformations of the DB anionic states of biomolecules, gaining deep insight into the mechanism of electron-induced biochemical processes.[2] The studies of DB cluster anions contribute significantly to understanding the structure of solute−solvent associates and the peculiarities of electron transfer reactions in solutions.[1e,g] The formation of DB states is thought to be the initial step in the attachment of an electron to many polar molecules.[2d,g,3]

Over many years, on the basis of ab initio and DFT calculations, the DB anion was considered as an unperturbed neutral molecule with an excess distant electron (its cloud is spatially diffuse and does not affect the nuclear core) localized on the positive side of the molecular dipole.[4] Experimental support for this view was seen in the corresponding anion photoelectron spectra (PES). As a rule, they were characterized by one intense, narrow peak, and the appearance of much weaker vibrational features was explained without involving the Franck−Condon overlap.[5]

The surprise was the photoelectron spectral signature of DB anions of H-bonded dimers, for example, $(HF)_2$,[5b,6a] $(H_2O)_2$,[6b] and $(H_2O{\cdot}NH_3)$.[6c] It was observed that the vibrational features in their PES resulted from a small shortening (<0.03 Å) of the intermolecular hydrogen bond upon attachment of an excess electron (EE).

In this context, seeking out and studying those "outlaw" dipole-bound anions that do not fit into the standard idea of the equivalence of geometries of the dipole-bound anions and their corresponding neutral molecules are of considerable interest.[7] Highly polar C_3 symmetrical intramolecular silicon complexes $XSi(OCH_2CH_2)_3N$, i.e., silatranes (**XS**), are ideal candidates for such investigation. It is pertinent to note that the existence of a labile dative Si ← N bond in **XS** molecules (Figure 1) predetermines their unique structure, unusual physical and chemical properties, as well as rich and various biological activities.[8−10] Mainly for this reason, the interest has not waned in the problem of the electronic structure of **XS**, its

Received: October 30, 2019
Published: January 3, 2020

https://dx.doi.org/10.1021/jacs.9b11694
J. Am. Chem. Soc. 2020, 142, 2001−2011

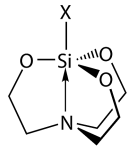

XS

X = Me (**MeS**), H (**HS**),
F (**FS**), Cl (**ClS**)

Figure 1. Silatrane molecules under investigation.

dependence on internal and external factors, and in the properties of the Si ← N coordination.[9b,10−13]

The combined experimental (Rydberg electron transfer and anion photoelectron spectroscopy, RET-PES) and theoretical (CCSD, CCSD(T), and MP2 computational methods) study revealed unprecedented shortening (by ∼0.1 Å) of the dative Si ← N bond upon the transition of 1-hydro- (**HS**) and 1-fluoro- (**FS**) silatranes to their dipole-bound anions, **HS**$^-$ and **FS**$^-$, respectively.[10] Furthermore, no vibrational features were observed in the photoelectron spectra of **HS**$^-$ and **FS**$^-$ anions, compared to that of the H-bonded dimers.[5b,6]

However, by the example of only two compounds **XS** (X = H, F) studied in ref 10, it is impossible to confidently answer some important questions. These include: (1) To what extent is a large structural rearrangement upon the EE "adhesion" also characteristic of other **XS** molecules? (2) What is the role, if any, of the substituent X in this case? (3) What properties of silatranes determine the unusual difference in the geometry of their DB anions and neutral molecules? (4) Is the formation of DB anions by highly polar cage molecules **XS** without the coordination Si ← N bond possible?

In view of the above, it became necessary to increase the number of the systems of investigation, i.e., to engage the other representatives of anions of **XS** in addition to **HS**$^-$ and **FS**$^-$.[10] We chose the anions of 1-methyl- (**MeS**) and 1-chlorosilatrane (**ClS**) (Figure 1). Judging by the dipole moment values in **XS**,[14] there is reason to believe that **MeS** has less ability and **ClS** has more ability to bind an EE compared with **HS** and **FS**, respectively.

2. COMPUTATIONAL METHODS

The geometries of the neutral molecules **XS** (X = Me, H, Cl, F) were optimized in the restricted variants of the second-order Møller−Plesset perturbation theory[15] (MP2/B2(s) method) and the coupled-cluster singles and doubles approach[16] (CCSD/6-31++G(d,p) and CCSD/6-311G(d,p) methods). The unrestricted variants of the MP2/B2(s) and CCSD/6-31++G(d,p) methods were applied for geometry optimizations of their dipole-bound anions **XS**$^-$ (more specifically, the radical-anions **XS**$^{-\bullet}$).

The B2(s)[10] basis set is a modification of the B2[17] basis set. The B2 basis set is constructed by augmenting the 6-311++G(d,p) basis set with a set of diffuse s and p functions. The exponents of these additional basis functions are obtained by dividing the smallest respective exponent of the 6-311++G(d,p) basis by a factor of 3 for oxygen, nitrogen, carbon, fluorine, chlorine, and silicon atoms and are taken to be equal to 0.001 for each hydrogen atom.[17] The B2(s) basis set differs from B2 by the addition of only s diffuse functions on hydrogen atoms.[10]

The correspondence of the MP2 and UMP2 optimized structures to the minima on the potential energy surface was confirmed by the positive eigenvalues of the corresponding Hessians. The neutral silatranes and their DB anions have only one minimum on the MP2/B2(s) potential energy surface.

The vertical electron detachment energy (VDE) is defined as the energy difference between the neutral molecule **XS** and its anion **XS**$^-$ both at the equilibrium geometry of the anion. The VDE estimations were performed using the CCSD and CCSD(T)[16,18] single-point calculations with the B2 basis set for the MP2/B2(s) geometries. The adiabatic electron affinity (AEA) was calculated as the CCSD(T)/B2 energy difference between the neutral species and its anion at their own MP2/B2(s) equilibrium geometries. Therewith, the corresponding contributions from the MP2/B2(s) vibrational zero-point energies (ZPE) were taken into account. No spin contamination was found for **XS**$^-$ when X = Me, H, F, Cl. The $\langle S^2 \rangle$ value is 0.750 in all cases.

Simulated photoelectron spectra of the dipole-bound anions **MeS**$^-$ and **ClS**$^-$ were generated with the Franck−Condon method[19,20] using the convolution of the MP2/B2(s) spectra with Gaussian distribution functions with a fwhm (full-width half-maximum) of 270 cm^{-1}.

All calculations were carried out using the Gaussian 09[21] program package.

Note that for studying **MeS**$^-$ and **ClS**$^-$, those methods that previously accurately reproduced the experimental VDE values as well as the PES profiles for **HS**$^-$ and **FS**$^-$ were utilized.[10]

Three-dimensional plots of the spin density were generated using the MOLDEN[22] program. The MOLEKEL[23] graphic software was implemented for visualizing the molecular electrostatic potential (MESP).

The AIM analysis[24] of the MP2/B2(s) electron density, $\rho(\mathbf{r})$, in silatranes **XS** and their DB anions was performed using the MORPHY1.0[25] and AIMAll[26] programs, as well as the BABBLE program from the AIMPAC[27] program package. On the contour plots of the laplacian of the electron density, $\nabla^2\rho(\mathbf{r})$, for **XS**$^-$ the contour values (in e/a_0^5) are ±0.002, ± 0.004, ± 0.008 increasing in powers of 10 to ±8.0 (the contours are shown in gray and correspond to the valence shell charge concentration) and ±8 × 10^{-4}, ± 4 × 10^{-4}, ± 2 ×

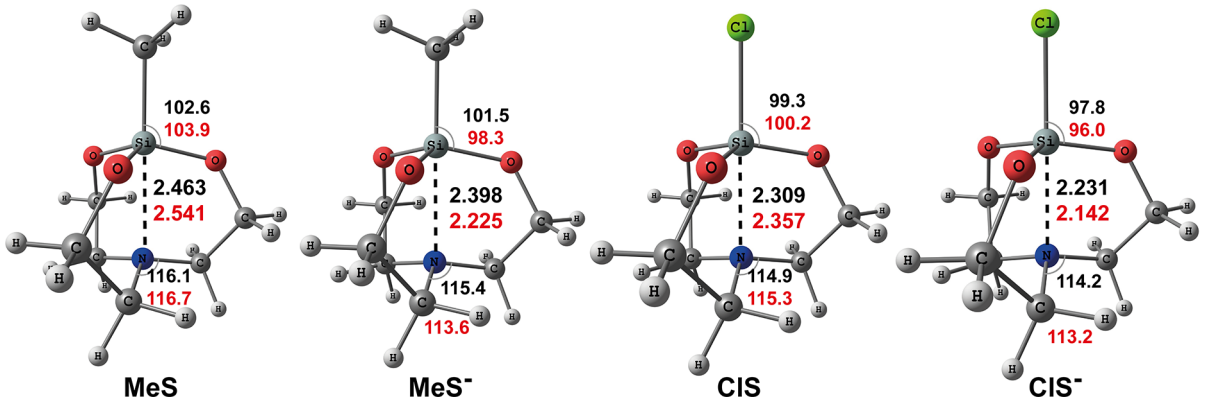

Figure 2. MP2/B2(s) (in black) and CCSD/6-31++G(d,p) (in red) optimized geometries of silatranes **MeS** and **ClS** and their dipole-bound anions **MeS**$^-$ and **ClS**$^-$. The bond lengths are in Å and the bond angles in degrees.

https://dx.doi.org/10.1021/jacs.9b11694
J. Am. Chem. Soc. 2020, 142, 2001−2011

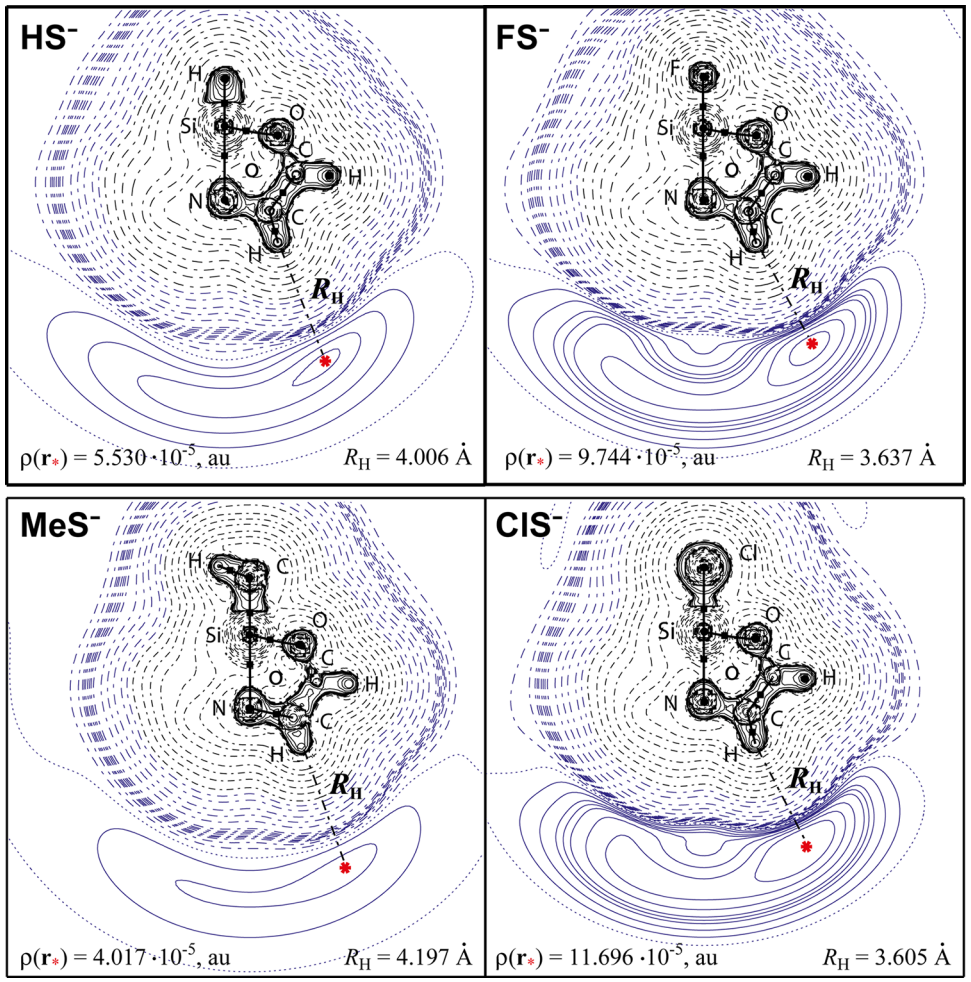

Figure 3. UMP2(full)/B2(s)//UMP2/B2(s) contour maps of $\nabla^2\rho(\mathbf{r})$ for the anions $\mathbf{XS}^-$. The cross section in the OSiN plane is given. Bond critical points, BCP(3,−1), of $\rho(\mathbf{r})$ are denoted by solid squares, and ring critical points, RCP(3,+1), by open cycles. Dashed lines correspond to $\nabla^2\rho(\mathbf{r}) > 0$ (regions of charge depletion) and solid lines to $\nabla^2\rho(\mathbf{r}) < 0$ (regions of charge concentration). The blue solid contours refer to DBCC. Red stars indicate the DBCC maxima.

10^{-4}, $\pm 8 \times 10^{-5}$, $\pm 4 \times 10^{-5}$, $\pm 2 \times 10^{-5}$, $\pm 9 \times 10^{-6}$, $\pm 7 \times 10^{-6}$, $\pm 6 \times 10^{-6}$, $\pm 5 \times 10^{-6}$, $\pm 4 \times 10^{-6}$, $\pm 3.5 \times 10^{-6}$, $\pm 3 \times 10^{-6}$, $\pm 2 \times 10^{-6}$, and $\pm 1 \times 10^{-6}$, given in blue (they correspond to the "dipole-bound" charge concentration).

The pentacoordinate character of the silicon atom, η_e, was determined with the aid of the relation:[28]

$$\eta_e = \left[1 - \frac{120 - 1/3\sum_{n=1}^{3}\theta_n}{120 - 109.5}\right] \times 100\% \quad (1)$$

Here, θ_n refer to the bond angle between the equatorial bonds at the silicon atom.

3. RESULTS AND DISCUSSION

3.1. Effect of Substituent X on the Structure of Silatrane DB Anions. The structural parameters, determined at the different theory levels for the neutral intramolecular complexes $XSi(OCH_2CH_2)_3N$ with X = Me, Cl, H, and F, have been repeatedly discussed in the literature.[8b,9d,10−13] Hence, there is no need for a detailed analysis of their structure.

Our MP2/B2(s), CCSD/6-311G(d,p), and CCSD/6-31++G(d,p) calculations of silatranes **MeS** and **ClS** (like those previously performed for **HS** and **FS**)[10] indicate the presence of the bonding Si ← N interaction in them (Figure 2, Table S1 of the Supporting Information, SI), which is in accordance with the known results.[8f,9d,11−13] This interaction manifests itself: (i) in the internuclear Si···N distances, d_{SiN}, which are substantially shorter than the sum of the van der Waals radii of Si and N (3.65 Å) and (ii) in the bond arrangement in the $XSiO_3N$ coordination center, being close to trigonal-bipyramidal and thereby in a large pentacoordinate character of the silicon atom, η_e (~50% and higher) (Table S1). The high η_e values and relatively short d_{SiN} are characteristic not only of **XS**, but also of the anions $\mathbf{XS}^-$ (Table S1).

With increasing the σ-acceptor properties of the substituent X in the direction:[29]

$$Me < H < Cl < F \quad (2)$$

the lengths of the Si ← N contacts in **XS** decrease, whereas the η_e values consistently increase (Figure 2 and Table S1). It turned out that such regularities of changes in d_{SiN} and η_e upon variation of X hold also for the anions $\mathbf{XS}^-$ (see Table S1). The reason for this is their DB nature.

Indeed, the spin density in $\mathbf{MeS}^-$ and $\mathbf{ClS}^-$, as in the case of $\mathbf{HS}^-$ and $\mathbf{FS}^-$,[10] is localized outside the nuclear framework (the immanent property of DB anions)[1e,4a,c] and therefore practically does not affect the σ-acceptor properties of the substituent X (Figures 3 and S1).

https://dx.doi.org/10.1021/jacs.9b11694
J. Am. Chem. Soc. 2020, 142, 2001−2011

Table 1. Dipole Moment (μ, D) of the Neutral Silatrane Molecules XS and Vertical Electron Detachment Energy (VDE, eV) for Their Anions XS^-

	calculation method	X = Me	X = H	X = F	X = Cl
μ	MP2/B2(s)	5.15	6.27	8.32	8.45
	CCSD/6-311G(d,p)	4.76	5.78	7.81	8.14
	CCSD/6-31++G(d,p)	4.86	6.06	8.36	8.60
VDE	UCCSD/B2//UMP2/B2(s)	0.027	0.045[a]	0.094[a]	0.108
	UCCSD(T)/B2//UMP2/B2(s)	0.029	0.048[a] (0.048)[a]	0.097[a] (0.093)[a]	0.112

[a]Previously calculated and experimentally obtained (shown in parentheses) VDE values.[10]

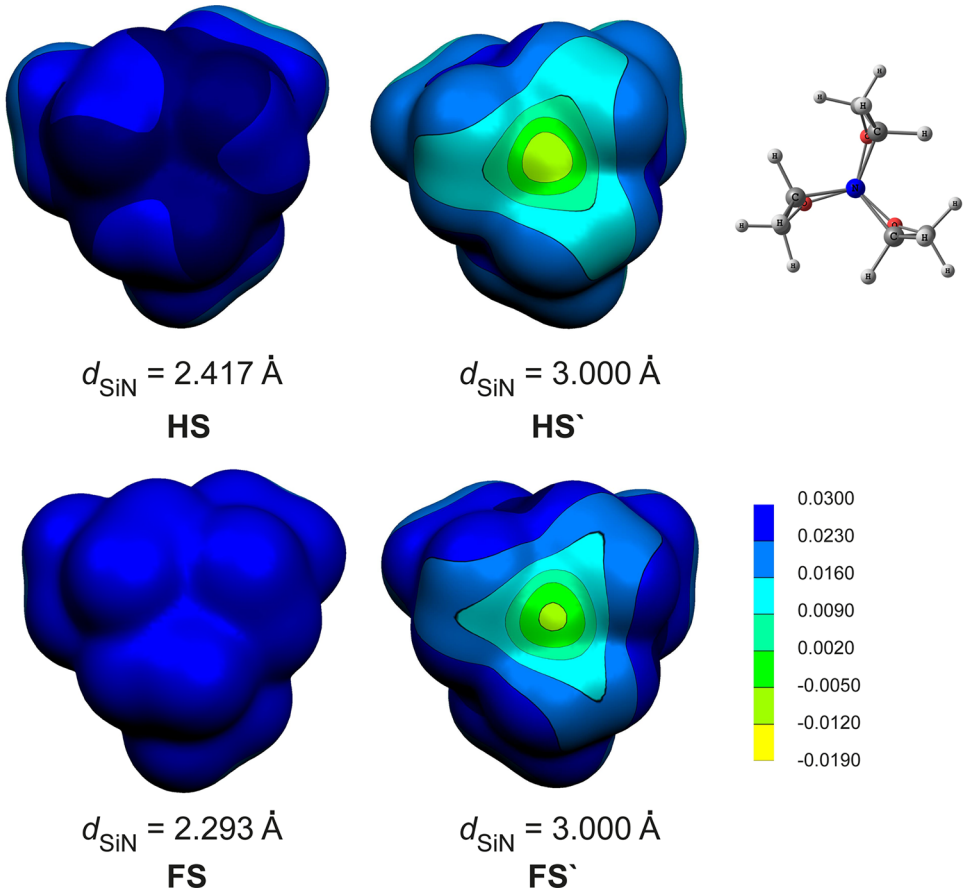

Figure 4. 3D representations of the CCSD/6-31++G(d,p) electrostatic potentials for silatranes **HS**, **FS**, and model structures **HS**$^/$ and **FS**$^/$, mapped on their isodensity surfaces (with isovalue of 0.0008 au). The MESPs are shown from the side of the $N(CH_2)_3$ moiety.

At a quantitative level, the dependence of the location and concentration of the EE cloud in XS^- on the properties of exocyclic substituent X can be evident from the AIM analysis of the electron density, $\rho(\mathbf{r})$. On the contour plots of the laplacian of the electron density, $\nabla^2\rho(\mathbf{r})$, for the anions XS^-, the excess electron gives rise to a very diffuse region of charge concentration (Figure 3), more so than that of the parent molecules **XS**. This region is defined as the "dipole-bound" charge concentration region (DBCC), as it is typical of the electron distribution in DB anions.[30] Inside this region, the critical points CP(3,−3) were found, corresponding to the maximum of DBCC (local minimum of $\nabla^2\rho(\mathbf{r})$).

The AIM analysis of the electronic density $\rho(\mathbf{r})$ revealed a (3,−1) bond critical point in the internuclear Si···N region of silatrane anions (Figure 3). This is a quantum topological support for the above geometrical evidence of the presence of Si ← N bond in XS^-.[24] A similar agreement between the AIM and structural indications of the silicon atom pentacoordination has been reported previously for neutral **XS**.[13b]

Upon variation of X, the distances R_H from the DBCC maxima to the nearest H atom (Figure 3) of the $N(CH_2)_3$ moiety in XS^- decrease as follows:

$$\mathbf{MeS^-} > \mathbf{HS^-} > \mathbf{FS^-} > \mathbf{ClS^-} \quad (3)$$

The values of $\rho(\mathbf{r})$ and $\nabla^2\rho(\mathbf{r})$ in CP(3,−3) change in a consistent manner with R_H, i.e., the closer the excess electron is located to the molecular framework, the higher will be the concentration of its cloud (Sequence 3, Figure 3, Table S2).

However, regardless of the theory level, the dipole moment, μ, in the series of **XS** increases in the sequence (Table 1):

$$\mathbf{MeS} < \mathbf{HS} < \mathbf{FS} < \mathbf{ClS} \quad (4)$$

Comparing sequences 3 and 4, one can see the non-accidental character of the changes in R_H and μ with varying X. The higher the polarity of the initial silatrane, the lower the R_H value becomes.

https://dx.doi.org/10.1021/jacs.9b11694
J. Am. Chem. Soc. 2020, 142, 2001−2011

On the basis of the DB nature of the anions $\mathbf{XS}^-$, one could expect a good relationship between the dipole moment of neutral compounds **XS** not only with R_H but also with the vertical electron detachment energies (VDE) for $\mathbf{XS}^-$. Indeed, with an increase in μ, both the above-mentioned shortening of the R_H distances and an increase in VDE are observed (Table 1). Moreover, the VDE values calculated at the CCSD/B2 and CCSD(T)/B2 levels of the theory are in excellent agreement with each other, and for the $\mathbf{HS}^-$ and $\mathbf{FS}^-$ anions also with the available experimental data.

Judging by the d_{SiN} values (Table S1), among the considered intramolecular complexes **XS** 1-methylsilatrane is characterized by the weakest coordination Si ← N bond. Moreover, the VDE value (0.029 eV) for its anion $\mathbf{MeS}^-$ turned out to be the smallest as well (Table 1).

In a large series of **XS**,[8b,f,9e] one can find compounds in which, for certain X, the Si ← N bond is weaker than in **MeS**, or it is essentially destroyed. However, they can be highly polar. Do such cage silatranes retain the capability to form DB anions? Unfortunately, this important question is hard to answer theoretically, since involving the real **XS** without the Si ← N bond (see refs 9e and 31,) poses a technical problem of the high-level VDE calculations of such large molecules.[10] However, the exceptional role of the Si ← N coordination in silatranes for the formation of their DB anions can be demonstrated by the example of model structures without the Si ← N bond, which contain a close to planar or planar NC_3 moiety (for $d_{SiN} \approx 3$ Å, the displacement of the N atom from the plane of three neighboring carbon atoms, $\Delta_N \approx 0$[32]). For such geometry of **XS**, no meaningful electronic and quantum topological signs of the Si ← N coordination are observed.

The CCSD/6-31++G(d,p) structure $\mathbf{HS}^{/}$ without bond (fixed d_{SiN} = 3.00 Å), constructed from the 1-hydrosilatrane molecule, is highly polar. For this structure, the μ value (3.39 D) is much larger than the "critical" dipole moment ($\mu \approx 2.5$ D) being necessary for the excess electron binding.[33] Nevertheless, the negative VDE values, which were calculated for the anion $\mathbf{HS}^{/-}$ at the UCCSD/B2//CCSD/6-31++G(d,p) and UCCSD/B2//MP2/B2(s) theory levels (−0.004 and −0.006 eV, respectively), are indicative of its instability.

Involving a map of the molecular electrostatic potential, MESP, might offer an explanation for this unusual result (Figure 4). For the equilibrium structures **XS** with the Si ← N bond, the positive end of the molecular dipole, i.e., the $N(CH_2)_3$ moiety, has a pyramidal structure that favors an effective shielding of the negative charge of the nitrogen atom by the positively charged CH_2 groups (Figure 5). For the planar structure of $N(CH_2)_3$ in $\mathbf{HS}^{/}$, the degree of such shielding is significantly reduced. And, as a result, on its MESP map there appears a region of the repulsive potential between an electron and a polar molecule (Figure 4), which prevents the formation of a stable dipole-bound state of $\mathbf{HS}^{/}$.

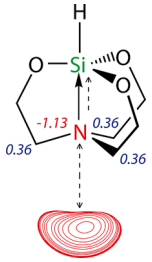

Figure 5. Schematic representation of the interaction between the $N(CH_2)_3$ moiety and a cloud of an excess electron in 1-hydrosilatrane. Numbers in italics show the atomic charge of nitrogen (in red) and the total charges of CH_2 groups (in blue) found by the AIM method at the MP2(full)/B2(s)//MP2/B2(s) level of theory.

The ability of structures without the Si ← N bond to form DB anions is retained if their polarity is significantly higher than that of $\mathbf{HS}^{/}$. For example, the CCSD/6-31++G(d,p) structure of 1-fluorosilatrane with an almost flat $N(CH_2)_3$ moiety (fixed d_{SiN} = 3.00 Å), $\mathbf{FS}^{/}$, is much more polar (μ = 5.08 D) than $\mathbf{HS}^{/}$. For this reason, even though the conditions are not very favorable for EE "adhesion" to the $\mathbf{FS}^{/}$ structure (Figure 4), its dipole-bound anion state is quite stable as judged by the positive value of its VDE (0.016 eV; UCCSD/B2//UCCSD/6-31++G(d,p)). However, this VDE value is essentially less than expected for μ = 5.08 D (see Table 1).

Thus, the formation of the cage DB anions of $XSi(OCH_2CH_2)_3N$ has principal features. It is controlled not only by the "critical" value of the dipole moment (μ > 2.5 D) but also by the geometric factor. Such a geometric factor is a degree of pyramidality of the $N(CH_2)_3$ moiety—the positive end of the molecular dipole of **XS**.

3.2. Effect of an Additional Electron on the Structure of Intramolecular Complexes XS. Upon the addition of an excess electron not only to silatranes **HS** and **FS**,[10] but also to **MeS** and **ClS**, a significant change in their structure is observed (Figure 2 and Table S1).

In quantitative terms, the transition from **XS** to $\mathbf{XS}^-$ had a most impressive effect on the length of the relatively weak coordination Si ← N bond. An AIM estimate of its energy gave ∼9 kcal/mol for **MeS** and ∼16 kcal/mol for **FS**.[13b] Therefore, as a measure of the silatrane geometry response to the EE addition, we chose the value $\Delta d_{SiN}(\mathbf{XS}) = d_{SiN}(\mathbf{XS}) - d_{SiN}(\mathbf{XS}^-)$. Regardless of the X substituent properties and the geometry optimization method, the Si ← N contact in $\mathbf{XS}^-$ is always shorter than in **XS**, i.e., $d_{SiN}(\mathbf{XS}) > d_{SiN}(\mathbf{XS}^-)$ (Figure 2 and Table S1).

The results of the performed calculations allowed us to suggest (using the example of **HS**) the following explanation for this fact. The EE cloud is located near the positive end of the silatrane molecular dipole, which corresponds to the $N(CH_2)_3$ moiety (Figures 3, 4, and S1). In this moiety, the nitrogen atom has a negative charge, while the CH_2 groups are positively charged (Figure 5). The local repulsion of N from the EE cloud leads to a displacement of this atom from the plane of three neighboring carbons in the direction of the silicon atom (MP2/B2(s): $\Delta_N(\mathbf{HS}) = 0.32$ Å, $\Delta_N(\mathbf{HS}^-) = 0.34$ Å; CCSD/6-31++G(d,p)): $\Delta_N(\mathbf{HS}) = 0.31$ Å, $\Delta_N(\mathbf{HS}^-) = 0.38$ Å) and, thereby, to a shortening of the Si ← N bond, i.e., to the inequality: $d_{SiN}(\mathbf{XS}) > d_{SiN}(\mathbf{XS}^-)$.

The $\Delta d_{SiN}(\mathbf{XS})$ value depends strongly on the theory level, basis set size and the X substituent nature. It is difficult to choose a priori the most reliable and cost-effective method for its estimation. Indeed, the available experimental electron diffraction (ED) Si ← N bond lengths in neutral **XS**[11c,34] are reproduced with good accuracy only by the CCSD method (depending on the basis size, the CCSD mean absolute error, MAE, is 0.009−0.021 Å,[10,12] while for the MP2/B2(s) calculations MAE = 0.052 Å[10]). On the contrary, there are serious reasons to believe that the UMP2/B2(s) optimized geometries for $\mathbf{XS}^-$ are much more reliable compared to the CCSD geometries obtained with the 6-31++G(d,p) and 6-311++G(d,p) basis sets.[10] The standard valence-type basis sets

https://dx.doi.org/10.1021/jacs.9b11694
J. Am. Chem. Soc. 2020, 142, 2001−2011

without extra diffuse functions are apparently not flexible enough for studying DB anions.[35] For these reasons, in the framework of one of the used theory levels, we cannot estimate the $\Delta d_{SiN}(\mathbf{XS})$ values relatively correctly. In this situation, two different methods have to be applied: ED (as in ref 10) or CCSD for obtaining $d_{SiN}(\mathbf{XS})$ and UMP2/B2(s) for calculating $d_{SiN}(\mathbf{XS}^-)$. Due to the lack of ED data for 1-chlorosilatrane[14b] and their poor quality for 1-methylsilatrane,[12,36] we will estimate the $d_{SiN}(\mathbf{XS})$ values using the CCSD method with the 6-311G(d,p) basis set. With this basis set (as compared to others), the best agreement is achieved between the calculated and available ED values of $d_{SiN}(\mathbf{XS})$ (MAE = 0.009).[12]

Thus, upon the transition from **XS** to $\mathbf{XS}^-$, the Si ← N bond deformation, i.e., the value of $\Delta d_{SiN}(\mathbf{XS}) = d_{SiN}[\mathbf{XS}]^{CCSD/6\text{-}311G(d,p)} - d_{SiN}[\mathbf{XS}^-]^{UMP2/B2(s)}$, decreases in the following sequence of substituent X:

$$\mathrm{Cl}(0.15\text{Å}) > \mathrm{Me}(0.13\text{Å}) > \mathrm{H}(0.12\text{Å}) > \mathrm{F}(0.10\text{Å}) \quad (5)$$

Judging by the $\Delta d_{SiN}(\mathbf{XS})$ values, the largest structural rearrangement upon EE "adhesion" to intramolecular complexes **XS** is characteristic of **ClS**. It significantly exceeds that for **HS**, which previously was a record for all DB anions known from the literature![10] Among the considered **XS** structures, 1-chlorosilatrane, **ClS**, is characterized by the highest polarity and, as a consequence, by the maximum interaction of EE with the **XS** framework (see Table 1). Therefore, it does not seem surprising that under the influence of EE the change in the geometry of **ClS** is greater than that of **MeS**, **HS**, and **FS** (see Sequence 5). Staying within the framework of such notions and based on the data of Table 1, we cannot answer the following question: Why is the effect of EE on the **XS** structure less pronounced in the case of **FS** (Sequence 5) than for **MeS** and **HS**? It appeared that this might be explained by the possible dependence of $\Delta d_{SiN}(\mathbf{XS})$ on the strength of the coordination Si ← N bond in the parent silatrane. The larger the internuclear Si···N distance, $d_{SiN}(\mathbf{XS})$, in **XS**, the more it would be subject to shortening during the transition from **XS** to $\mathbf{XS}^-$. However, in general, a satisfactory correlation between $\Delta d_{SiN}(\mathbf{XS})$ and $d_{SiN}(\mathbf{XS})$ is not observed in the series of **XS**.

According to the CCSD/6-31++G(d,p) calculations, the dipole moment is equal to 4.86 and 8.36 D for the equilibrium geometries of **MeS** and **FS**, respectively, and μ = 6.99 and 9.45 D when using the corresponding geometries of their DB anions. At any theory level and regardless of the nature of the substituent X, the polarity of silatranes with the anionic geometry is higher than with the optimized geometry of neutral **XS**. Ultimately, this contributes to the enhancement of the EE interaction with the intramolecular complexes **XS**. Such an effect has been previously observed during the formation of DB anions of intermolecular complexes stabilized by a hydrogen[6] or N → B[7] bond.

Thus, the structural rearrangement of **XS**, initiated by EE "adhesion" to these molecules, proceeds in the direction of the increase of their polarity. This is accompanied, first of all, by a significant shortening of the dative Si ← N contact (see sequence 5). Therefore, there is reason to expect that the greater the deformation of the coordination Si ← N bond, $\Delta d_{SiN}(\mathbf{XS})$, in silatranes, the greater is the rate ($V\mu$) of increase of the dipole moment of **XS** with decreasing the internuclear Si···N distance. The rate $V\mu$ is defined as follows:[37]

$$V\mu = |(\mu_{eq} - \mu_1)/(d_{eq} - d_1)| \quad (6)$$

where μ_{eq} and d_{eq} correspond to the optimized geometry of silatrane, and μ_1 is determined at its Si ← N bond length, d_1, which differs from the equilibrium bond length, d_{eq}, by a relatively small arbitrary constant c ($d_1 < d_{eq}$).

The foregoing is supported by the CCSD/6-311G(d,p) calculations of $V\mu$ for **XS** (for definiteness c = 0.005 Å). When X varies, the $V\mu$ values (in D/Å) decrease in the following sequence that does not depend on the value of the constant c:

$$\mathrm{Cl}(5.54) > \mathrm{Me}(4.56) > \mathrm{H}(4.36) > \mathrm{F}(3.78) \quad (7)$$

Comparing sequences 5 and 7, we can see that indeed $\Delta d_{SiN}(\mathbf{XS})$ and $V\mu$ change in concert in the series of **XS** (see Figure 6).

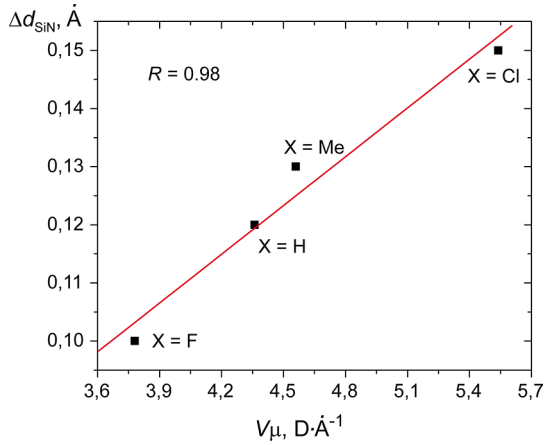

Figure 6. Dependence of the Si ← N bond deformation initiated by EE in silatranes **XS** on the rate of increase of their dipole moment with decreasing the internuclear Si···N distance.

Thus, the sensitivity of the geometry of silatranes to the EE effect is controlled by the rate of increase of their dipole moment with the shortening of the Si ← N contact, $V\mu$.

3.3. Photoelectron Spectra of DB Silatrane Anions.

The photoelectron spectra of anions $\mathbf{MeS}^-$ and $\mathbf{ClS}^-$ simulated with the Franck–Condon method (Figure 7 and Tables S3 and S4) are similar to those for $\mathbf{HS}^-$ and $\mathbf{FS}^-$.[10] The geometric relaxation upon the EE attachment occurs mainly along the first and seventh normal vibrational modes in **MeS** and along the first and sixth modes in **ClS**. As in the case of **HS** and **FS**,[10] they correspond to the dative Si ← N bond stretching and torsional motion of the SiO_3 and $N(CH_2)_3$ moieties around the C_3 symmetry axis in the silatrane molecule. The vibrational transitions (0_0^0, 1_0^1, 7_0^1) and (0_0^0, 1_0^1 6_0^1) are very close in energy (see the ΔE values in Tables S3 and S4) and form a separate, narrow main peak in PES of $\mathbf{MeS}^-$ and $\mathbf{ClS}^-$, being typical of dipole bound anions.[4]

In addition to a separate intense maximum, very weak vibrational features appear around 0.4 eV ($\mathbf{MeS}^-$) and 0.5 eV ($\mathbf{ClS}^-$) (Figure 7), which is in contrast to the theoretical PES of the $\mathbf{HS}^-$ and $\mathbf{FS}^-$ molecules.[10] They have a composite character and correspond to transitions related largely to stretching of different C–H bonds of the silatrane cage. These combination bands also involve the torsional motion of the methyl group in the case of $\mathbf{MeS}^-$ and the O–Si–O bending and CH_2 group twisting for $\mathbf{ClS}^-$. Judging by the Franck–Condon factors values (Tables S3 and S4) these peaks (especially at 0.5 eV) have a very low intensity and are

https://dx.doi.org/10.1021/jacs.9b11694
J. Am. Chem. Soc. 2020, 142, 2001–2011

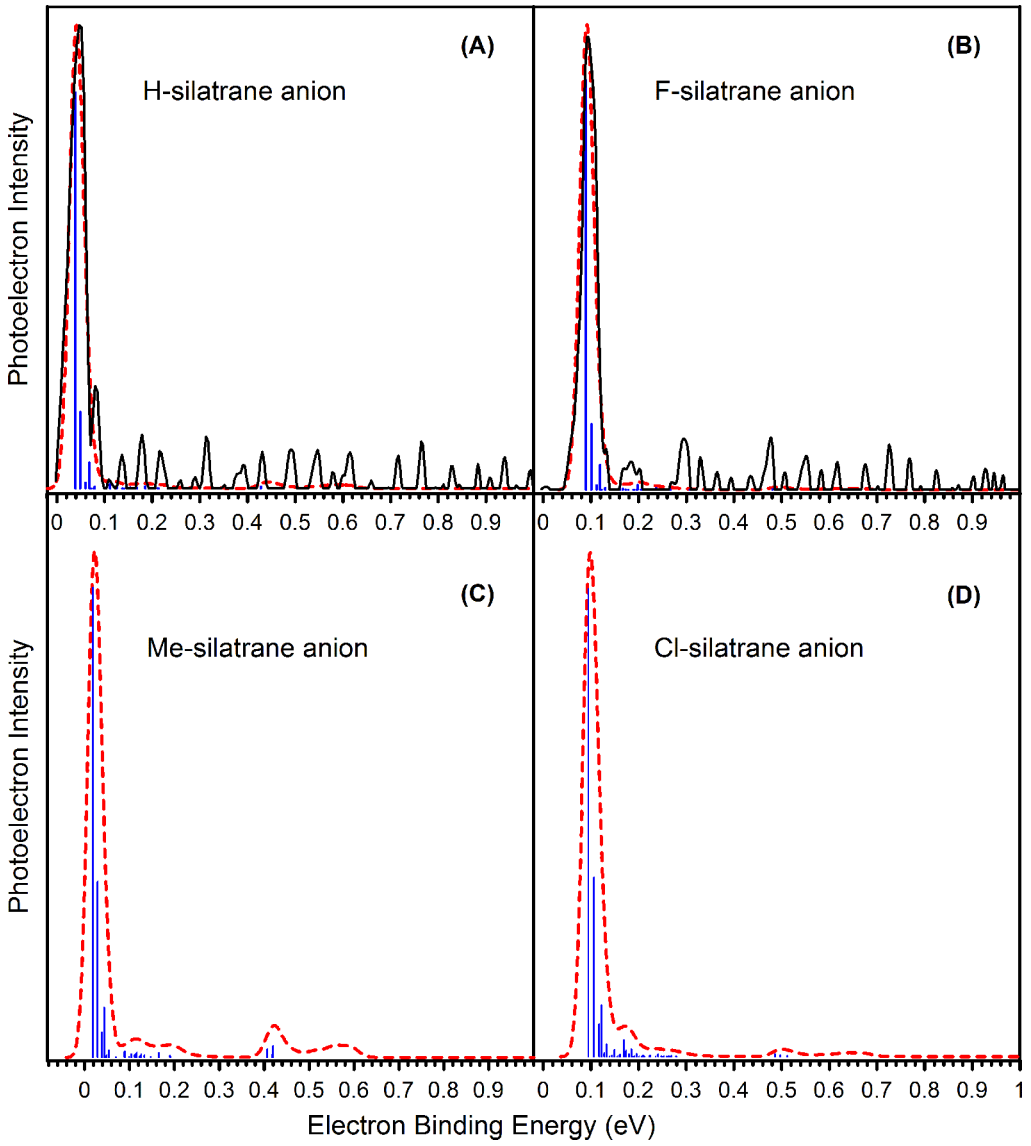

Figure 7. (A,B) Overlaid experimental (RET-PES, black solid line) and Franck−Condon (red dashed line) photoelectron spectra of $\mathbf{HS}^-$ and $\mathbf{FS}^-$. (C,D) Theoretical photoelectron spectra of anions $\mathbf{MeS}^-$ and $\mathbf{ClS}^-$. Vibrational progressions are given by a blue line spectrum. The geometry optimizations and normal vibrational mode calculations were performed with the MP2/B2(s) method. In determining the position of the 0−0 transition we used the CCSD(T)/B2 adiabatic electron affinity values (19 meV for **MeS** and 95 meV for **ClS**). Panels A,B reprinted with permission from Belogolova, E. F., et al. *J. Phys. Chem. Lett.*, 9, 1284−1289.

practically not populated upon the electron photodetachment from $\mathbf{MeS}^-$ and $\mathbf{ClS}^-$.

Thus, in PES of silatrane anions there is no vibrational structure (Figure 7 and Tables S3 and S4), which could be considered as evidence of an unprecedented deformation of the coordination Si ← N bond (see Section 3.2). This surprising fact is largely due to its striking lability.[38] Indeed, according to the CCSD(T) calculations, only ∼0.02 eV of energy is required to change the Si ← N distance by 0.1 Å.[10] Therefore, the vibrational transitions that correspond to the deformation of the $XSiO_3$ ← $N(CH_2)_3$ moiety do not go beyond the limits of a narrow main peak in PES of anions $\mathbf{XS}^-$ (see Figure 7 and Tables S3 and S4).

It is important to note that the vibrational structure observed in the photoelectron spectra of the anions of intermolecular H-complexes, for example $(HF)_2$, is largely due to the peculiarities of the H-bond deformation, namely, its significant bending and small (<0.03 Å) stretching.[6a,c] On the contrary, because of the lateral stiffness of the silatrane cage (with respect to the axial XSi ← N plane), we have a zero Franck−Condon factor for the coordination Si ← N bond bending in $\mathbf{XS}^-$.

On the basis of the results of ref 10, an unusual photoelectron spectrum can be expected for the anions of those silatranes, which would be characterized by an *extraordinary* Si···N distance shortening (Δd_{SiN} > 0.2 Å (!)) during the process **XS** → $\mathbf{XS}^-$.

There is no real reason to doubt that the peculiarities of the formation of DB anions of intramolecular complexes $XSi(OCH_2CH_2)_3N$ with a cage structure (discussed above in sections 3.1 and 3.2) can be characteristic, but with surprises, also for many hundreds of their structural analogues $XM(YCH_2CH_2)_3N$ (M = Si, Ge, Sn, Pb, Ti, Al, Cr, Fe, Ni...; Y = O, NR, CH_2, S) - substituted 5-azabicyclo[3.3.3]undecans.

https://dx.doi.org/10.1021/jacs.9b11694
J. Am. Chem. Soc. 2020, 142, 2001−2011

4. CONCLUSIONS

The MP2, CCSD, CCSD(T), and AIM methods were applied to study the structure and energetics of the formation of dipole-bound, DB, anions of intramolecular silicon complexes—silatranes $XSi(OCH_2CH_2)_3N$, **XS** (X = Me, H, F, Cl), which possess the dative Si ← N bond.

The DB character of the silatrane anions $\mathbf{XS}^-$ is proven by the localization of their spin density outside the nuclear framework and by the appearance of the "dipole-bound" charge concentration region on the corresponding contour plots of the laplacian of the electron density. The "adhesion" of an excess electron, EE, to **XS** is always accompanied by a shortening of the coordination Si ← N bond. This can be explained by the local repulsion between EE and the negatively charged nitrogen atom of the $N(CH_2)_3$ moiety, which is the positive end of the silatrane molecular dipole. The dissimilarity in the structure of **ClS** and $\mathbf{ClS}^-$ (determined mainly by the difference in the internuclear Si···N distance, which is equal to 0.15 Å(!)) is a record for all DB anions known from the literature.

The regularities of changes in the structural parameters of the Si ← N coordination upon variation of X, which were established for neutral **XS**, hold also for the anions $\mathbf{XS}^-$. The Si ← N interaction in these molecules strengthens with increasing σ-acceptor properties of the axial substituent X (Me < H < Cl < F).

According to the calculations, the higher the polarity, μ, of the parent silatrane, the closer the electron cloud is to the molecular framework, and the higher is its concentration. An increase in μ in the series of **XS** (**MeS** < **HS** < **FS** < **ClS**) also results in the expected increase in the vertical electron detachment energy of the corresponding anions ($\mathbf{MeS}^-$ < $\mathbf{HS}^-$ < $\mathbf{FS}^-$ < $\mathbf{ClS}^-$).

The formation of DB anions of **XS** with the cage structure is controlled not only by the "critical" value of the dipole moment (μ > 2.5 D), as in the case of usual structures, but also by the geometric factor. Such a geometric factor is the degree of pyramidality of the $N(CH_2)_3$ moiety—the positive end of the molecular dipole of **XS**.

The observed effect of the substituent X on the structural rearrangement in the process **XS** → $\mathbf{XS}^-$ cannot be explained using the values of the electron detachment energy of $\mathbf{XS}^-$ or the initial strength of the Si ← N bond in **XS**.

The sensitivity of the geometry of silatranes to the addition of an excess electron, which do not fit into the standard views, is governed by the rate of increase of their dipole moment with the shortening of the Si ← N contact.

A more significant effect of EE on the structure of **MeS** and **ClS** (as compared to that of **HS** and **FS**) was not noticeably manifested in the Franck–Condon photoelectron spectra of their anions.

■ ASSOCIATED CONTENT

Supporting Information

The Supporting Information is available free of charge on the ACS Publications Web site at DOI: The Supporting Information is available free of charge at https://pubs.acs.org/doi/10.1021/jacs.9b11694.

Figure S1 with spin density distribution for the dipole-bound anions of 1-chloro-, 1-fluoro-, 1-hydro-, and 1-methylsilatrane; Table S1 with the calculated structural parameters of four silatranes and their dipole-bound anions; Table S2 with the values of the electron density, and the laplacian of the electron density at the maxima of the dipole-bound charge concentration for silatrane anions; Tables S3 and S4 with the Franck–Condon factors, intensities, and transition energies in the photoelectron spectra of the 1-methyl- and 1-chlorosilatrane anions; and Cartesian coordinates of all the stationary points (PDF)

■ AUTHOR INFORMATION

Corresponding Authors

Valery F. Sidorkin − *Siberian Branch of the Russian Academy of Sciences, Irkutsk, Russian Federation;* orcid.org/0000-0002-8848-7567; Email: svf@irioch.irk.ru

Kit H. Bowen − *Johns Hopkins University, Baltimore, Maryland;* orcid.org/0000-0002-2858-6352; Email: kbowen@jhu.edu

Other Authors

Elena F. Belogolova − *Siberian Branch of the Russian Academy of Sciences, Irkutsk, Russian Federation;* orcid.org/0000-0001-5599-1778

Evgeniya P. Doronina − *Siberian Branch of the Russian Academy of Sciences, Irkutsk, Russian Federation;* orcid.org/0000-0001-6663-061X

Gaoxiang Liu − *Johns Hopkins University, Baltimore, Maryland;* orcid.org/0000-0002-1001-0064

Sandra M. Ciborowski − *Johns Hopkins University, Baltimore, Maryland;* orcid.org/0000-0001-9453-4764

Complete contact information is available at: https://pubs.acs.org/10.1021/jacs.9b11694

Notes

The authors declare no competing financial interest.

■ ACKNOWLEDGMENTS

The experimental part of this material is based upon work supported by the U.S. National Science Foundation (NSF) under grant number, CHE-1952511. We are grateful to Prof. P. L. A. Popelier for a copy of the MORPHY1.0 program, the Irkutsk Supercomputer Center of SB RAS for providing computational resources of the computational cluster "Academician V. M. Matrosov"[39] to perform the topological analysis of the molecules under study.

■ REFERENCES

(1) (a) Jordan, K. D. Studies of the Temporary Anion States of Unsaturated Hydrocarbons by Electron Transmission Spectroscopy. *Acc. Chem. Res.* **1979**, *12* (1), 36–42. (b) Simons, J.; Jordan, K. D. Ab Initio Electronic Structure of Anions. *Chem. Rev.* **1987**, *87* (3), 535–555. (c) Gutowski, G.; Skurski, P.; Boldyrev, A. I.; Simons, J.; Jordan, K. D. Contribution of Electron Correlation to the Stability of Dipole-Bound Anionic States. *Phys. Rev. A: At., Mol., Opt. Phys.* **1996**, *54* (3), 1906–1909. (d) Compton, R. N.; Hammer, N. I. Multipole-bound molecular anions. *Adv. Gas Phase Ion Chem.* **2001**, *4*, 257–305. (e) Simons, J. Molecular Anions. *J. Phys. Chem. A* **2008**, *112* (29), 6401–6511. (f) Liu, H. T.; Ning, C. G.; Huang, D. L.; Dau, P. D.; Wang, L. S. Observation of Mode-Specific Vibrational Autodetachment from Dipole-Bound States of Cold Anions. *Angew. Chem., Int. Ed.* **2013**, *52* (34), 8976–8979. (g) Zhang, Y.; Weber, P. M.; Jonsson,

H. Self-Interaction Corrected Functional Calculations of a Dipole-Bound Molecular Anion. *J. Phys. Chem. Lett.* **2016**, *7* (11), 2068−2073. (h) Ciborowski, S. M.; Liu, G.; Graham, J. D.; Buytendyk, A. M.; Bowen, K. H. Dipole-bound anions: formed by Rydberg electron transfer (RET) and studied by velocity map imaging−anion photoelectron spectroscopy (VMI−aPES). *Eur. Phys. J. D* **2018**, *72* (8), 139.

(2) (a) Hendricks, J. H.; Lyapustina, S. A.; de Clercq, H. L.; Snodgrass, J. T.; Bowen, K. H. Dipole bound, nucleic acid base anions studied via negative ion photoelectron spectroscopy. *J. Chem. Phys.* **1996**, *104* (19), 7788−7791. (b) Hendricks, J. H.; Lyapustina, S. A.; de Clercq, H. L.; Bowen, K. H. The dipole bound-to-covalent anion transformation in uracil. *J. Chem. Phys.* **1998**, *108* (1), 8−11. (c) Schiedt, J.; Weinkauf, R.; Neumark, D. M.; Schlag, E. W. Anion spectroscopy of uracil, thymine and the amino-oxo and amino-hydroxy tautomers of cytosine and their water clusters. *Chem. Phys.* **1998**, *239* (1−3), 511−524. (d) Sommerfeld, T. Intramolecular Electron Transfer from Dipole-Bound to Valence Orbitals: Uracil and 5-Chlorouracil. *J. Phys. Chem. A* **2004**, *108* (42), 9150−9154. (e) Sommerfeld, T. Dipole-bound states as doorways in (dissociative) electron attachment. *J. Phys.: Conf. Ser.* **2005**, *4*, 245−250. (f) Burrow, P. D.; Gallup, G. A.; Scheer, A. M.; Denifl, S.; Ptasinska, S.; Märk, T.; Scheier, P. Vibrational Feshbach resonances in uracil and thymine. *J. Chem. Phys.* **2006**, *124* (12), 124310−7. (g) Liu, G.; Ciborowski, S. M.; Pitts, C. R.; Graham, J. D.; Buytendyk, A. M.; Lectka, T.; Bowen, K. H. Observation of the dipole- and quadrupole-bound anions of 1,4-dicyanocyclohexane. *Phys. Chem. Chem. Phys.* **2019**, *21* (33), 18310−18315.

(3) (a) Sommerfeld, T. Doorway Mechanism for Dissociative Electron Attachment to Fructose. *J. Chem. Phys.* **2007**, *126* (12), 124301−124305. (b) Eustis, S. N.; Radisic, D.; Bowen, K. H.; Bachorz, R. A.; Haranczyk, M.; Schenter, G.; Gutowski, M. Electron-Driven Acid Base Chemistry: Proton Transfer from Hydrogen Chloride to Ammonia. *Science* **2008**, *319* (5865), 936−939. (c) Chomicz, L.; Zdrowowicz, M.; Kasprzykowski, F.; Rak, J.; Buonaugurio, A.; Wang, Y.; Bowen, K. H. How to Find Out Whether a 5-Substituted Uracil Could Be a Potential DNA Radiosensitizer. *J. Phys. Chem. Lett.* **2013**, *4* (17), 2853−2857. (d) Liu, G.; Ciborowski, S. M.; Graham, J. D.; Buytendyk, A. M.; Bowen, K. H. The ground state, quadrupole-bound anion of succinonitrile revisited. *J. Chem. Phys.* **2019**, *151* (10), 101101−5. (e) Ciborowski, S. M.; Harris, R. M.; Liu, G.; Martinez-Martinez, C. J.; Skurski, P.; Bowen, K. H. The correlation-bound anion of p-chloroaniline. *J. Chem. Phys.* **2019**, *150* (16), 161103−4.

(4) (a) Jordan, K. D.; Luken, W. Theoretical Study of the Binding of an Electron to a Molecular Dipole: $LiCl^-$. *J. Chem. Phys.* **1976**, *64* (7), 2760−2766. (b) Chipman, D. M. Theoretical study on the electron affinity of the water dimer. *J. Phys. Chem.* **1979**, *83* (12), 1657−1662. (c) Barnett, R. N.; Landman, U.; Cleveland, C. L.; Jortner, J. Electron localization in water clusters. II. Surface and internal states. *J. Chem. Phys.* **1988**, *88* (7), 4429−4447. (d) Gutsev, G. L.; Sobolewski, A. L.; Adamowicz, L. A theoretical study on the structure of acetonitrile (CH_3CN) and its anion CH_3CN^-. *Chem. Phys.* **1995**, *196* (1−2), 1−11. (e) Gutsev, G. L.; Adamowicz, L. Electronic and geometrical structure of dipole-bound anions formed by polar molecules. *J. Phys. Chem.* **1995**, *99* (36), 13412−13421. (f) Castleman, A. W.; Bowen, K. H. Clusters: Structure, Energetics, and Dynamics of Intermediate States of Matter. *J. Phys. Chem.* **1996**, *100* (31), 12911−12944.

(5) (a) Bailey, C. G.; Dessent, C. E. H.; Johnson, M. A.; Bowen, K. H., Jr. Vibronic effects in the photon energy-dependent photoelectron spectra of the CH_3CN^- dipole-bound anion. *J. Chem. Phys.* **1996**, *104* (18), 6976−6983. (b) Hendricks, J. H.; de Clercq, H. L.; Lyapustina, S. A.; Bowen, K. H. Negative Ion Photoelectron Spectroscopy of the Ground State, Dipole-Bound Dimeric Anion, $(HF)_2^-$. *J. Chem. Phys.* **1997**, *107* (8), 2962−2967.

(6) (a) Gutowski, M.; Skurski, P. Theoretical Study of the Dipole-Bound Anion $(HF)_2^-$. *J. Chem. Phys.* **1997**, *107* (8), 2968−2973. (b) Bouteiller, Y.; Desfrançois, C.; Abdoul-Carime, H.; Schermann, J. P. Structure and intermolecular motions of the water dimer anion. *J. Chem. Phys.* **1996**, *105* (15), 6420−6425. (c) Skurski, P.; Gutowski, M. Theoretical study of the dipole-bound anion $(H_2O\cdots NH_3)^-$. *J. Chem. Phys.* **1998**, *108* (15), 6303−6311.

(7) (a) Barrios, R.; Skurski, P.; Rak, J.; Gutowski, M. An ab initio study of $(H_3B{\leftarrow}NH_3)^-$ − a dipole-bound anion supported by the dative charge-transfer bond in the neutral host. *J. Chem. Phys.* **2000**, *113* (20), 8961−8968. (b) Sawicka, A.; Skurski, P. Dipole-bound anions supported by charge-transfer interaction: valence- and dipole-bound anionic states of $H_3N{\rightarrow}BF_3$. *Chem. Phys.* **2002**, *282* (3), 327−336. (c) Sawicka, A.; Anusiewicz, I.; Skurski, P.; Simons, J. Dipole-bound anions supported by charge−transfer interaction: Anionic states of $H_nF_{3-n}N \rightarrow BH_3$ and $H_3N \rightarrow BH_nF_{3-n}$ (n = 0, 1, 2, 3). *Int. J. Quantum Chem.* **2003**, *92* (4), 367−375.

(8) (a) Verkade, J. G. Main group atranes: chemical and structural features. *Coord. Chem. Rev.* **1994**, *137*, 233−295. (b) Pestunovich, V.; Kirpichenko, S.; Voronkov, M. Silatranes and their tricyclic analogs. In *The Chemistry of Organic Silicon Compounds*; Rappoport, Z., Apeloig, Y., Eds.; Wiley: 1998; Vol. 2, Chapter 2, pp 1447−1537. (c) Shlyakhtenko, L. S.; Gall, A. A.; Filonov, A.; Cerovac, Z.; Lushnikov, A.; Lyubchenko, Y. L. Silatrane-based surface chemistry for immobilization of DNA, protein-DNA complexes and other biological materials. *Ultramicroscopy* **2003**, *97* (1−4), 279−287. (d) Yadav, G. D.; Manyar, H. G. Converting liability into asset: Novel mesoporous zeotype from fly ash using silatrane chemistry. *Clean Technol. Environ. Policy* **2005**, *7* (3), 162−167. (e) D'yakov, V. M.; Voronkov, M. G.; Kazimirovskaya, V. B.; Loginov, S. V.; Rasulov, M. M. Wound healing effects of some silocanes and silatranes. In *Organosilicon Chemistry VI: For Molecules to Materials*; Auner, N., Weis, J., Eds.; Wiley-VCH Verlag GmbH: 2008; Chapter 4, pp 588−594. (f) Puri, J. K.; Singh, R.; Chahal, V. K. Silatranes: A Review on Their Synthesis, Structure, Reactivity and Applications. *Chem. Soc. Rev.* **2011**, *40* (3), 1791−1840. (g) Singh, G.; Sanchita; Singh, A.; Sharma, G.; Kalra, P.; Satija, P.; Diksha; Soni, S.; Verma, V. Ester appended organosilatranes: Paradigm for the detection of Cu^{2+}, Pb^{2+} and Hg^{2+} ion. *Inorg. Chim. Acta* **2019**, *490*, 85−92.

(9) (a) Peureux, C.; Jouikov, V. Covalent Grafting of Silatranes to Carbon Interfaces. *Chem. - Eur. J.* **2014**, *20* (30), 9290−9294. (b) Belogolova, E. F.; Vakul'skaya, T. I.; Sidorkin, V. F. Radical Anions of Hypervalent Silicon Compounds: 1-Substituted Silatranes. *Phys. Chem. Chem. Phys.* **2015**, *17*, 12735−12746. (c) Romanovs, V.; Sidorkin, V.; Belogolova, E.; Jouikov, V. Radical cations of phenyl silatrane. *Dalton Trans.* **2017**, *46*, 8849−8854. (d) Sidorkin, V. F.; Belogolova, E. F.; Wang, Y.; Jouikov, V.; Doronina, E. P. Electrochemical Oxidation and Radical Cations of Structurally Non-Rigid Hypervalent Silatranes: Theoretical and Experimental Studies. *Chem. - Eur. J.* **2017**, *23*, 1910−1919. (e) Meshgi, M. A.; Zitz, R.; Walewska, M.; Baumgartner, J.; Marschner, C. Tuning the Si−N Interaction in Metalated Oligosilanylsilatranes. *Organometallics* **2017**, *36* (7), 1365−1371.

(10) Belogolova, E. F.; Liu, G.; Doronina, E. P.; Ciborowski, S. M.; Sidorkin, V. F.; Bowen, K. H. Dipole-Bound Anions of Intramolecular Complexes. *J. Phys. Chem. Lett.* **2018**, *9*, 1284−1289.

(11) (a) Kobayashi, J.; Goto, K.; Kawashima, T.; Schmidt, M. W.; Nagase, S. Synthesis, Structure, and Bonding Properties of 5-Carbaphosphatranes: A New Class of Main Group Atrane. *J. Am. Chem. Soc.* **2002**, *124* (14), 3703−3712. (b) Korlyukov, A. A.; Lyssenko, K. A.; Antipin, M. Y.; Kirin, V. N.; Chernyshev, E. A.; Knyazev, S. P. Experimental and Theoretical Study of the Trans-annular Intramolecular Interaction and Cage Effect in the Atrane Framework of Boratrane and 1-Methylsilatrane. *Inorg. Chem.* **2002**, *41* (20), 5043−5051. (c) Shishkov, I. F.; Khristenko, L. V.; Rudakov, F. M.; Golubinskii, A. V.; Vilkov, L. V.; Karlov, S. S.; Zaitseva, G. S.; Samdal, S. Molecular Structure of Silatrane Determined by Gas Electron Diffraction and Quantum-Mechanical Calculations. *Struct. Chem.* **2004**, *15* (1), 11−16. (d) Dillen, J. A Quantum Mechanical Investigation of the Nature of the Dative Bond in Crystalline 1-Chlorosilatrane. *J. Phys. Chem. A* **2004**, *108* (22), 4971−4977. (e) Trofimov, A. B.; Zakrzewski, V. G.; Dolgounitcheva, O.; Ortiz, J. V.; Sidorkin, V. F.; Belogolova, E. F.; Belogolov, M.; Pestunovich, V.

https://dx.doi.org/10.1021/jacs.9b11694
J. Am. Chem. Soc. 2020, 142, 2001−2011

A. Silicon-Nitrogen Bonding in Silatranes: Assignment of Photoelectron Spectra. *J. Am. Chem. Soc.* **2005**, *127* (3), 986−995. (f) Zabalov, M. V.; Karlov, S. S.; Zaitseva, G. S.; Lemenovskii, D. A. The molecular and electronic structure features of silatranes, germatranes, and their carbon analogs. *Russ. Chem. Bull.* **2006**, *55* (3), 464−476. (g) Ignatyev, I. S.; Sundius, T. R.; Vrazhnov, D. V.; Kochina, T. A.; Voronkov, M. G. Bonding in germatranyl cation and germatranes. *J. Organomet. Chem.* **2007**, *692* (26), 5697−5700.

(12) Belogolova, E. F.; Sidorkin, V. F. Correlation Among the Gas-Phase, Solution, and Solid-Phase Geometrical and NMR Parameters of Dative Bonds in the Pentacoordinate Silicon Compounds. 1-Substituted Silatranes. *J. Phys. Chem. A* **2013**, *117* (25), 5365−5376.

(13) (a) Korlyukov, A. A. Coordination compounds of tetravalent silicon, germanium and tin: the structure, chemical bonding and intermolecular interactions in them. *Russ. Chem. Rev.* **2015**, *84* (4), 422−440. (b) Sidorkin, V. F.; Belogolova, E. F.; Doronina, E. P. Assignment of Photoelectron Spectra of Silatranes: First Ionization Energies and the Nature of the Dative Si←N Contact. *Phys. Chem. Chem. Phys.* **2015**, *17*, 26225−26237. (c) Marín-Luna, M.; Alkorta, I.; Elguero, J. Theoretical study of the geometrical, energetic and NMR properties of atranes. *J. Organomet. Chem.* **2015**, *794*, 206−215. (d) Hoeksema, C.; Adler, M. J.; Gilbert, T. M. Computational Study of Ways by Which exo-Silatranes Might Be Prepared. *J. Phys. Chem. A* **2016**, *120* (46), 9315−9323. (e) Morgan, J. P.; Weaver-Guevara, H. M.; Fitzgerald, R. W.; Dunlap-Smith, A.; Greenberg, A. Ab initio computational study of l-methyl-4-silatranone and attempts at its conventional synthesis. *Struct. Chem.* **2017**, *28* (2), 327−331. (f) Belogolova, E. F.; Doronina, E. P.; Sidorkin, V. F. Assignment of photoelectron spectra of intramolecular silicon complexes: 1-vinyl- and 1-phenylsilatranes. *Phys. Chem. Chem. Phys.* **2018**, *20*, 26210−26220.

(14) (a) Hencsei, P.; Csonka, G.; Zsombok, G.; Gergő, É. Calculation of dipole moments for silatranes. *Period. Polytech., Chem. Eng.* **1983**, *27* (4), 263−268. (b) Csonka, G. I.; Hencsei, P. The Structure of 1-Chlorosilatrane: An Ab Initio Molecular Orbital and a Density Functional Theory Study. *J. Comput. Chem.* **1996**, *17* (7), 767−780.

(15) (a) Møller, C.; Plesset, M. S. Note on an approximation treatment for many-electron systems. *Phys. Rev.* **1934**, *46* (7), 618−622. (b) Head-Gordon, M.; Pople, J. A.; Frisch, M. J. MP2 energy evaluation by direct methods. *Chem. Phys. Lett.* **1988**, *153* (6), 503−506. (c) Head-Gordon, M.; Rico, R. J.; Oumi, M.; Lee, T. J. A Doubles Correction to Electronic Excited-States from Configuration-Interaction in the Space of Single Substitutions. *Chem. Phys. Lett.* **1994**, *219* (1−2), 21−29.

(16) (a) Čížek, J. On the Use of the Cluster Expansion and the Technique of Diagrams in Calculations of Correlation Effects in Atoms and Molecules. *Adv. Chem. Phys.* **2007**, *14*, 35−89. (b) Purvis, G. D.; Bartlett, R. J. A full coupled-cluster singles and doubles model: The inclusion of disconnected triples. *J. Chem. Phys.* **1982**, *76* (4), 1910−1918. (c) Scuseria, G. E.; Janssen, C. L.; Schaefer, H. F. An efficient reformulation of the closed-shell coupled cluster single and double excitation (CCSD) equations. *J. Chem. Phys.* **1988**, *89* (12), 7382−7387.

(17) Streit, L.; Dolgounitcheva, O.; Zakrzewski, V. G.; Ortiz, J. V. Valence and Diffuse-Bound Anions of Noble-Gas Complexes with Uracil. *J. Chem. Phys.* **2012**, *137* (19), 194310−10.

(18) Pople, J. A.; Head-Gordon, M.; Raghavachari, K. Quadratic configuration interaction - a general technique for determining electron correlation energies. *J. Chem. Phys.* **1987**, *87* (10), 5968−5975.

(19) (a) Franck, J.; Dymond, E. G. Elementary processes of photochemical reactions. *Trans. Faraday Soc.* **1926**, *21*, 536−542. (b) Condon, E. U. Nuclear Motions Associated with Electron Transitions in Diatomic Molecules. *Phys. Rev.* **1928**, *32* (6), 858−872.

(20) (a) Santoro, F.; Improta, R.; Lami, A.; Bloino, J.; Barone, V. Effective method to compute Franck-Condon integrals for optical spectra of large molecules in solution. *J. Chem. Phys.* **2007**, *126* (8), 084509−13. (b) Santoro, F.; Lami, A.; Improta, R.; Barone, V. Effective method to compute vibrationally resolved optical spectra of large molecules at finite temperature in the gas phase and in solution. *J. Chem. Phys.* **2007**, *126* (18), 184102−9. (c) Santoro, F.; Lami, A.; Improta, R.; Bloino, J.; Barone, V. Effective method for the computation of optical spectra of large molecules at finite temperature including the Duschinsky and Herzberg−Teller effect: The *Qx* band of porphyrin as a case study. *J. Chem. Phys.* **2008**, *128* (22), 224311−16.

(21) Frisch, M. J.; Trucks, G. W.; Schlegel, H. B.; Scuseria, G. E.; Robb, M. A.; Cheeseman, J. R.; Scalmani, G.; Barone, V.; Mennucci, B.; Petersson, G. A.; Nakatsuji, H.; Caricato, M.; Li, X.; Hratchian, H. P.; Izmaylov, A. F.; Bloino, J.; Zheng, G.; Sonnenberg, J. L.; Hada, M.; Ehara, M.; Toyota, K.; Fukuda, R.; Hasegawa, J.; Ishida, M.; Nakajima, T.; Honda, Y.; Kitao, O.; Nakai, H.; Vreven, T.; Montgomery, J. A., Jr.; Peralta, J. E.; Ogliaro, F.; Bearpark, M.; Heyd, J. J.; Brothers, E.; Kudin, K. N.; Staroverov, V. N.; Keith, T.; Kobayashi, R.; Normand, J.; Raghavachari, K.; Rendell, A.; Burant, J. C.; Iyengar, S. S.; Tomasi, J.; Cossi, M.; Rega, N.; Millam, J. M.; Klene, M.; Knox, J. E.; Cross, J. B.; Bakken, V.; Adamo, C.; Jaramillo, J.; Gomperts, R.; Stratmann, R. E.; Yazyev, O.; Austin, A. J.; Cammi, R.; Pomelli, C.; Ochterski, J. W.; Martin, R. L.; Morokuma, K.; Zakrzewski, V. G.; Voth, G. A.; Salvador, P.; Dannenberg, J. J.; Dapprich, S.; Daniels, A. D.; Farkas, O.; Foresman, J. B.; Ortiz, J. V.; Cioslowski, J.; Fox, D. J. *Gaussian 09*, Revision C.01; Gaussian, Inc.: Wallingford, CT, 2010.

(22) Schaftenaar, G. *MOLDEN 3.4*; CAOS/CAMM Center: The Netherlands, 1998, http://cheminf.cmbi.ru.nl/molden/.

(23) Portmann, S.; Flükiger, P. F.; Lüthi, H. P.; Weber, J. *Molekel 4.3*; University of Geneva and Swiss Center for Scientific Computing: Manno, Switzerland, 2002, http://www.cscs.ch/molkel/.

(24) Bader, R. F. W. *Atoms in Molecules: a Quantum Theory*; Clarendon Press: 1990.

(25) (a) Popelier, P. L. A. MORPHY, a program for an automated "atoms in molecules" analysis. *Comput. Phys. Commun.* **1996**, *93* (2−3), 212−240. (b) Popelier, P. L. A. A robust algorithm to locate automatically all types of critical points in the charge density and its Laplacian. *Chem. Phys. Lett.* **1994**, *228* (1−3), 160−164.

(26) Keith, T. A. *AIMAll (Version 14.06.21)*; TK Gristmill Software: Overland Park, KS, 2014, http://aim.tkgristmill.com.

(27) *AIMPAC*; McMaster University: Hamilton, ON, http://www.chemistry.mcmaster.ca/aimpac/.

(28) Tamao, K.; Hayashi, T.; Ito, Y.; Shiro, M. Pentacoordinate Anionic Bis(siliconates) Containing a Fluorine Bridge between Two Silicon Atoms. Synthesis, Solid-State Structures, and Dynamic Behavior in Solution. *Organometallics* **1992**, *11* (6), 2099−2114.

(29) Hencsei, P. Evaluation of silatrane structures by correlation relationships. *Struct. Chem.* **1991**, *2* (1), 21−26.

(30) (a) Timerghazin, Q. K.; Peslherbe, G. H. Non-nuclear attractor of electron density as a manifestation of the solvated electron. *J. Chem. Phys.* **2007**, *127* (6), 064108−4. (b) Timerghazin, Q. K.; Peslherbe, G. H. Electronic Structure of the Acetonitrile and Acetonitrile Dimer Anions: A Topological Investigation. *J. Phys. Chem. B* **2008**, *112* (2), 520−528.

(31) (a) Eaborn, C.; Odell, K. J.; Pidcock, A.; Scollary, G. R. A Silatrane-Platinum Complex, trans-/$PtClSi(OCH_2CH_2)_3N$-$(PMe_2Ph)_2$/, with a Planar Nitrogen and No Si-N Bond; X-Ray Crystal Structure. *J. Chem. Soc., Chem. Commun.* **1976**, *9*, 317−318. (b) Attar-Bashi, M. T.; Rickard, C. E. F.; Roper, W. R.; Wright, L. J.; Woodgate, S. D. Quaternization of the Bridgehead Nitrogen in Silatranylosmium(II) Complexes and Reestablishment of the Transannular N-Si Bond following Migratory Insertion of the Silatranyl Ligand. *Organometallics* **1998**, *17* (4), 504−506. (c) Rickard, C. E. F.; Roper, W. R.; Woodman, T. J.; Wright, L. J. The synthesis and crystal structure of the first metal-bound stannatrane complex $Os(Sn[OCH_2CH_2]_3N)(\eta^2\text{-}S_2CNMe_2)(CO)(PPh_3)_2$: structural comparisons with the analogous silatrane complex $Os(Si[OCH_2CH_2]_3N)(\eta^2\text{-}S_2CNMe_2)(CO)(PPh_3)_2$. *Chem. Commun.* **1999**, No. 9, 837−838. (d) Meshgi, M. A.; Baumgartner, J.; Marschner, C. Oligosilanylsilatranes. *Organometallics* **2015**, *34* (15), 3721−3731. (e) Meshgi, M. A.;

https://dx.doi.org/10.1021/jacs.9b11694
J. Am. Chem. Soc. 2020, 142, 2001−2011

Baumgartner, J.; Jouikov, V. V.; Marschner, C. Electron Transfer and Modification of Oligosilanylsilatranes and Related Derivatives. *Organometallics* **2017**, *36* (2), 342−351.
(32) Greenberg, A.; Wu, G. Structural relationships in silatrane molecules. *Struct. Chem.* **1990**, *1* (1), 79−85.
(33) (a) Crawford, H. O.; Dalgarno, A. Bound states of an electron in a dipole field. *Chem. Phys. Lett.* **1967**, *1* (1), 23−23. (b) Desfrançois, C.; Abdoul-Carime, H.; Schermann, J. P. Ground-state dipole-bound anions. *Int. J. Mod. Phys. B* **1996**, *10* (12), 1339−1395. (c) Qian, C.-H.; Zhu, G.-Z.; Wang, L.-S. Probing the Critical Dipole Moment To Support Excited Dipole-Bound States in Valence-Bound Anions. *J. Phys. Chem. Lett.* **2019**, *10*, 6472−6477.
(34) Forgacs, G.; Kolonits, M.; Hargittai, I. The Gas-Phase Molecular Structure of 1-Fluorosilatrane from Electron Diffraction. *Struct. Chem.* **1990**, *1* (2−3), 245−250.
(35) Skurski, P.; Gutowski, M.; Simons, J. How to Choose a One-Electron Basis Set to Reliably Describe a Dipole-Bound Anion. *Int. J. Quantum Chem.* **2000**, *80*, 1024−1038.
(36) Shen, Q.; Hilderbrandt, R. L. The structure of methylsilatrane (1-methyl-2,8,9-trioxa-5-aza-1-silabicyclo(3.3.3)undecane) as determined by gas phase electron diffraction. *J. Mol. Struct.* **1980**, *64* (34), 257−262.
(37) Doronina, E. P.; Sidorkin, V. F.; Lazareva, N. F. (PO→Si) Chelates of Silylmethyl Derivatives of Phosphoric Acids $R_2P(O)$-$ZCH_2SiMe_{3-n}Hal_n$ (n = 1−3; Z = O, NMe, CH_2, S). *Organometallics* **2010**, *29* (15), 3327−3340.
(38) (a) Sidorkin, V. F.; Doronina, E. P. Cage Silaphosphanes with a P-Si Dative Bond. *Organometallics* **2009**, *28* (18), 5305−5315. (b) Csonka, G. I.; Hencsei, P. Ab Initio Molecular Orbital Study of 1-Fluorosilatrane. *J. Comput. Chem.* **1994**, *15* (4), 385−394. (c) Schmidt, M. W.; Windus, T. L.; Gordon, M. S. Structural Trends in Silicon Atranes. *J. Am. Chem. Soc.* **1995**, *117* (28), 7480−7486.
(39) Irkutsk Supercomputer Center of SB RAS; *ISDCT SB RAS*; Irkutsk: http://hpc.icc.ru, accessed September 2019.

https://dx.doi.org/10.1021/jacs.9b11694
J. Am. Chem. Soc. 2020, 142, 2001−2011